n-heptane reforming over Pt supported on beta zeolite exchanged with Cs and Li cations

S. Ramírez [a], M. Viniegra [a], J.M. Domínguez [b], P. Schacht [c] and Louis Ch. De Ménorval [d]

[a] *Departamento de Química, Universidad Autónoma Metropolitana-Iztapalapa, Av. Michoacán y Purísima s/n, México 09340 D.F., Mexico*
[b] *Instituto Mexicano del Petróleo, STI, Programa de Simulación Molecular, Eje Central L. Cárdenas 152, México 07730 D.F., Mexico*
[c] *Instituto Mexicano del Petroléo, Gerencia de Catalizadores, Eje Central L. Cárdenas 152, México 07730 D.F., Mexico*
[d] *Laboratoire de Matériaux Catalytiques et Catalyse en Chimie Organique, UMR-5618 ENSCM, CNRS, 8 rue de l'Ecole Normale, 34296 Montpellier Cédex 05, France*

Received 29 October 1999; accepted 26 January 2000

The physicochemical and catalytic properties of platinum supported on beta zeolite both acid and exchanged with Cs and Li cations were characterized by X-ray diffraction, NH_3-TPD, FTIR of adsorbed pyridine and CO, DSC, mass spectrometry and hydrogen chemisorption. The n-heptane conversion was performed to assess the selectivity variations in the exchanged solids. A high metal dispersion was verified in all of the catalysts, varying from 54 up to 81%. The FTIR of adsorbed CO revealed a shift towards lower frequencies for Pt on exchanged zeolite with respect to Pt on the acid zeolite, indicating that the basic character of Cs and Li enhance the electron donation from the support to the metal. The acid–base properties of the exchanged materials influence their selectivity for the catalytic conversion of n-heptane at 663 K and 1 atm, showing that Cs promotes the aromatization reactions while Li promotes isomerization and cracking. The cracking activity followed the acid/metal ratio for all of the catalysts studied.

Keywords: Pt, beta zeolite, ion exchange, n-heptane reforming

1. Introduction

The interest of studying zeolitic materials as possible systems for gasoline upgrading processes started soon after the results published by Bernard [1] at the beginning of the eighties, showing an increment in the aromatization of n-hexane by platinum supported on KL zeolite. This is interesting for industrial processes such as reforming [2] and C_5–C_6 hydroisomerization [3] among others. The high aromatization and isomerization levels obtained with platinum supported on beta zeolite, either in the acid form or exchanged with alkaline metals, are among the best results. Smirniotis and coworkers [4] found that a catalyst formulated with 0.5 wt% platinum supported on beta zeolite (ZβH) showed a higher selectivity for skeletal isomerization reactions, in comparison with the catalyst of platinum supported on alumina. They assumed that this is a result of the closer vicinity among the bifunctional active sites of the catalyst. Similar results were reported by Yue Chu et al. [5], indicating a selectivity towards the isomerization of n-hexane of 99% over Pt/ZβH catalysts. The addition of alkaline cations to the zeolite supports was reported by Zheng and coworkers [6] who found that platinum supported on beta zeolite exchanged with cesium showed important increments in the aromatization of n-hexane. More recently, Bécue et al. [7] obtained similar results using platinum supported on beta zeolite exchanged with sodium and cesium. Fukunaga and Ponec [8] also reported higher levels of aromatization of n-heptane with these systems. Blomsma, Martens and Jacobs [9,10] have studied the mechanism of the n-heptane conversion on platinum and palladium supported on beta zeolite in its acid form. They have established that these reactions can occur by means of both, a classical and a dimerization mechanism.

The results obtained in the aromatization and isomerization of hydrocarbons in the gasoline boiling range have encouraged the research on platinum supported on beta zeolite with the aim of using it as a reforming catalyst. The low-temperature isomerization properties of Pt/ZβH catalysts are of industrial interest for the reforming of the gasoline cut. However, the high acidity of the zeolitic supports decreases the yield of high-octane gasoline and hydrogen, producing higher proportions of light gas and alkenes [11].

In this way, our interest was to study the properties of a reforming bifunctional catalyst based on platinum supported on beta zeolite, both acid (Pt/ZβH) and exchanged with Cs and Li cations (Pt/ZβCs and Pt/ZβLi). Several characterization techniques were employed to assess the main properties of the solids, namely: number of acid sites by TPD-NH_3 and FTIR of adsorbed pyridine. The decomposition of the metallic salt was followed by differential scanning calorimetry (DSC), and mass spectrometry while hydrogen chemisorption was performed to determine the metal dispersion. FTIR of adsorbed CO and the catalytic n-heptane reforming were employed to test the chemical behavior of the solids. The evaluation of Pt/Al_2O_3 and a commercial Pt/Al_2O_3–Cl catalyst was included for comparison purposes.

2. Experimental

2.1. Preparation of catalysts

2.1.1. Materials

Beta zeolite in its acid form, having a sodium content of less than 100 ppm (Valfor CP811Bl-75), was obtained from PQ Corporation and was used without further treatment. The specifications are: molar Si/Al ratio = 33, 85% crystallinity, 742 m^2/g of surface area and a pore volume of 0.18 cm^3/g. The precursors for the alkaline cations were monohydrated LiOH from Rosemount, and CH_3CO_2Li and CsOH from Aldrich. The source of platinum was $Pt(NH_3)_4(NO_3)_2$ (Aldrich) and the solution prepared contained 1018 ppm of metal, as determined by atomic absorption spectroscopy (AAS).

2.1.2. Ion exchange

The general procedure for the ion exchange [12] consisted in adding the proper amounts of the Cs or Li solution to the zeolite suspended in water. The pH variation was continuously registered and this mixture was kept under slow agitation overnight at room temperature. The samples were filtered and dried in two steps, the first one at 313 K and the second one at 393 K, then they were calcined at 823 K during 2 h. The exchange level was calculated from the total aluminum content determined by AAS, as reported in table 1.

For the deposition of platinum, the supports were dried in a reactor with flowing air at 393 K for 2 h. The proper amount of platinum solution was then added and this solution was maintained in slow agitation overnight. In some cases, small amounts of NH_4OH were added to the mixture in order to keep the pH at ca. 6. Then, the solid was filtered and washed with deionized water. The drying step was carried out as described above. The solids were calcined in a fixed-bed reactor with an air flow of 120 cm^3/min at 623 K during 2 h. Finally, the reduction step was performed under flowing hydrogen (120 cm^3/min) at 623 K during 2 h.

The catalysts were labeled according to:

(a) Pt/Zβ H: platinum supported on beta zeolite (acid form).

(b) Pt/Zβ Cs, Pt/Zβ Li1 and Pt/Zβ Li2: platinum supported on beta zeolites exchanged with Cs and Li, respectively.

(c) GAPt1: platinum supported on γ-alumina.

The last sample was prepared for comparison purposes and it was synthesized by ion exchange with a high-purity γ-alumina (Kali Chemie) and platinum(II) acetyl acetonate (Aldrich) in toluene solution. The procedure of drying was made as described above. The reference was a commercial catalyst (CatCom) from the Instituto Mexicano del Petróleo (0.375 wt% Pt on alumina and 1 wt% of chlorine).

2.2. Apparatus and procedures

The elemental analysis was carried out by AAS in a Perkin–Elmer spectrometer model 2380. It included the quantification of cesium, lithium, silicon, aluminum, platinum and other elements such as iron, copper and sodium.

The dispersion of platinum was determined by hydrogen chemisorption at room temperature in a home-made, grease-free, volumetric apparatus. Before recording the adsorption isotherms, the samples were pretreated at the reduction temperature in hydrogen for 1 h and degassed at the same temperature overnight. Then, the temperature was lowered to 293 K, and the adsorption isotherms were recorded.

The conditions for oxidation and reduction were determined by means of the thermal decomposition analysis followed with mass spectrometry (MS). These analyses were made in a modified DSC-PE7 apparatus, with flowing air (for the oxidation) or a mixture of 5% hydrogen in argon (for the reduction) in a quartz cell loaded with a small amount of catalyst. The heat released during the treatment process, from room temperature up to 793 K, was measured by differential scanning calorimetry (DSC) and the identification of the decomposition products from both reactions was made on line by MS.

2.3. Number of acid sites

The number of acid sites was determined by NH_3-TPD using a thermal conductivity detector fitted to a GC (Gow

Table 1
Composition, Pt dispersion and acid properties of Pt/beta zeolite catalysts.

Sample	Cation (wt%)	Exchange level (wt%)	Pt (wt%)	Dispersion (%)	Platinum particle size[a] (Å)	Number of acid sites (μmol NH_3/g)
Zβ H	0.0	–	–	–	–	472
Pt/Zβ H	0.0	–	0.3952	75	13	462
Zβ Cs	6.44	97.7	–	–	–	71
Pt/Zβ Cs	6.44	97.7	0.3990	62	16	99
Zβ Li1	0.28	81.3	–	–	–	305
Pt/Zβ Li1	0.28	81.3	0.3701	81	12	377
Zβ Li2	0.33	110.4	–	–	–	260
Pt/Zβ Li2	0.33	110.4	0.4332	54	19	540
GAPt1	–	–	0.4049	75	13	370
CatCom	–	–	0.375	65	–	370

[a] Determined from the hydrogen adsorption data.

Mac series 580). The samples were pretreated under a helium flow of 2 l/h, from room temperature up to 923 K during 1.5 h. Anhydrous ammonia was injected by pulses, at 473 K, until saturation was achieved. Then, a helium flow was admitted and the temperature was decreased down to 413 K. The ammonia desorption was followed from 413 to 873 K with a heating rate of 10 K/min under flowing helium (2 l/h). The amount of NH_3 desorbed per gram of catalyst was determined from the area under the curve. The results are reported as μmol of NH_3 desorbed per gram of catalyst.

2.4. FTIR of adsorbed pyridine and CO

The nature of the acid sites was determined by FTIR spectroscopy of adsorbed pyridine using a Nicolet 170SX instrument. Self-supported wafers (13 mm of diameter) were introduced into a Pyrex glass cell with CaF_2 windows and were pretreated under vacuum (10^{-6} Torr) at 673 K for 1 h. The adsorption of 20 Torr of pyridine (Merck, spectrophotometric grade) was performed at room temperature during 30 min; then, the vapor-phase pyridine was vacuum removed at the same temperature for 30 min. The spectra were recorded at various temperatures, from 293 to 773 K. The integrated IR absorbance of the bands at 1545 cm^{-1} (Brønsted) and 1450 cm^{-1} (Lewis) were considered, and the transmission factors reported by Emeis [13] were used for the calculations.

The spectra of adsorbed CO were recorded at room temperature and 473 K on the samples reduced *in situ*. The self-supported wafers were treated under hydrogen flow overnight at 623 K. The temperature was decreased to room temperature and the samples were evacuated at 10^{-6} Torr. After the adsorption of 20 Torr of CO the spectra were collected over the samples evacuated at high vacuum (10^{-6} Torr).

2.5. Catalytic activity

The catalytic tests were made at atmospheric pressure and 663 K, using n-heptane as the reactant in a glass microreactor unit. The feed was a mixture of n-heptane (11.37 Torr) and hydrogen with a H_2/n-C_7 molar ratio of 50.5. The reactor had an internal diameter of 0.6 cm, and the bed was a porous glass fitted with a thermowell.

The product analysis was made with a gas chromatograph (Varian 3400 CX) fitted with a flame ionization detector and a capillary column of 60 m of length and 0.13 mm of diameter, applying a temperature program. The factors of Dietz [14] were used for the calculation of the product distribution. The transferring lines for hydrogen–hydrocarbon mixtures were fitted with heating tapes to avoid possible condensation.

The selectivity for each reforming reaction was calculated in terms of the products having seven carbon atoms and n-heptane converted as suggested by Rasser [15]:

(a) aromatization selectivity

$$S_{\mathrm{a}} = \frac{\text{aromatics}}{\text{products C}_7} \times 100;$$

(b) isomerization selectivity

$$S_{\mathrm{i}} = \frac{\text{branched alkanes}}{\text{products C}_7} \times 100;$$

(c) cyclization selectivity

$$S_{\mathrm{c}} = \frac{\text{cycloalkanes}}{\text{products C}_7} \times 100;$$

(d) cracking selectivity

$$S_{\mathrm{h}} = \frac{\text{cracked products}}{n\text{-C}_7 \text{ converted}} \times 100.$$

The hydrocarbons considered in the calculation of these selectivities were toluene (Tol) for aromatization; 2,2-dimethylpentane ($22dMC_5$), 2,3-dimethylpentane ($23dMC_5$), 2-methylhexane ($2MC_6$) and 3-methylhexane ($3MC_6$) for isomerization; ethylcyclopentane ($ECyC_5$) and methylcyclohexane ($MCyC_6$) for cyclization; ethane (C_2), propane (C_3) and butane (C_4) for the cracking reactions.

3. Results

3.1. Thermal analysis

During the calcination of Pt/ZβH the ion species corresponding to water, ammonia and nitrogen dioxide were identified with MS on line. The results showed that water and ammonia desorption, as well as the maximum formation of nitrogen oxides occurred at low temperatures, approximately at 643 K, decreasing above this temperature. Other authors [16] reported the decomposition of the platinum complex at 593 K as observed by FTIR. The DSC results showed the appearance of the main exothermic peak at 580 K corresponding to the formation of NO_x from the tetraammine platinum(II) nitrate. No further desorption of water was observed above 473 K.

The MS results obtained during the reduction of Pt/ZβH were followed taking into account the concentration of the compounds having molecular weights of 18, 17 and 46, i.e., water, ammonia and nitrogen dioxide, respectively. Water and ammonia were released from 443 to 703 K approximately. The results from the DSC analysis showed a peak at 350 K corresponding to the reduction of platinum species (probably PtO_2 [17]) to its metallic state. Based on these results, the temperature for both oxidation and reduction processes was fixed at 623 K.

3.2. Elemental analysis and platinum dispersion

The main properties of the ion-exchanged zeolites and catalysts are displayed in table 1.

The sample ZβCs was prepared by ion exchange of cesium hydroxide in solution, with a final concentration of

6.44 wt% Cs. The samples ZβLi1 and ZβLi2 were prepared by ion exchange with lithium acetate and lithium hydroxide, respectively. The third column of table 1 shows the exchange level for these zeolites; that is, the amount of cesium or lithium added in relation to the exchange capacity of the zeolite, which was calculated from the total aluminum content. The particle size determined from the chemisorption experiments varied slightly in the series, i.e., from 12 to 16 Å.

3.3. Number of acid sites

Table 1 shows the number of acid sites determined by NH_3-TPD. It is observed that the lowest figure corresponds to beta zeolite fully exchanged with Cs (71 μmol NH_3/g). The samples exchanged with Li have a substantially higher value, i.e., 305 μmol NH_3/g for ZβLi1 and 260 μmol NH_3/g for ZβLi2. The samples Pt/ZβCs, Pt/ZβLi1 and Pt/ZβLi2 increased their number of acid sites, after platinum addition, in 39, 23 and 107%, respectively.

The number of acid sites of ZβH matched the theoretical value calculated from the total content of Al in the zeolite, i.e., 472 vs. 496 μmol NH_3/g, respectively. This latter value was calculated considering that all of the Al atoms were accessible and located in the zeolite crystalline framework.

3.4. FTIR of adsorbed pyridine

Figures 1 and 2 show the Brønsted and total acid sites (Brønsted sites + Lewis sites) distribution determined by FTIR of pyridine adsorbed on the reduced catalysts.

Figure 1 shows the Brønsted acid sites distribution for ZβH, Pt/ZβH, ZβLi1 and Pt/ZβLi2 in the temperature range from 473 to 773 K. For the rest of the samples the number of Brønsted sites was zero; as expected, the highest number of Brønsted acid sites corresponded to ZβH. The number of Brønsted acid sites decreased after Pt exchange, i.e., for Pt/ZβH the change was −2.1%.

Figure 2 shows the total acid sites profile as a function of temperature for ZβH, Pt/ZβH, Pt/ZβCs, Pt/ZβLi1, Pt/ZβLi2 and GAPt1. The acid support (ZβH) had the highest population of acid sites. The catalysts Pt/ZβH and GAPt1 had about the same distribution however, the former presented Brønsted acid sites (figure 1). The catalyst exchanged with Cs had a number of acid sites lower than the catalysts exchanged with Li, and a high percentage of these sites were weak Lewis acid sites that desorb pyridine at temperatures lower than 473 K. The number of acid sites (Brønsted + Lewis) at 473 K followed the sequence:

$$\text{ZβH} > \text{Pt/ZβLi2} > \text{Pt/ZβCs} \approx \text{Pt/ZβLi1} > \text{Pt/ZβH} = \text{GAPt1}.$$

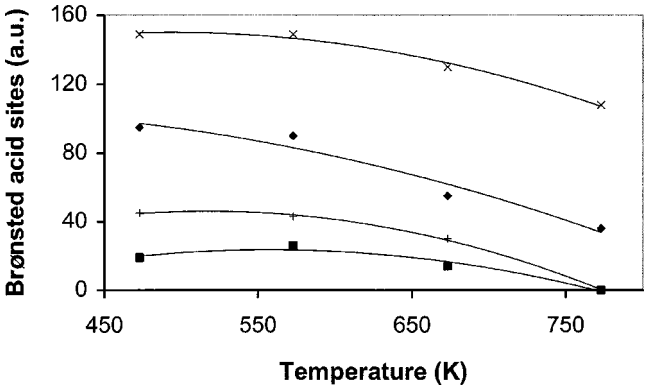

Figure 1. Brønsted acid sites distribution determined by FTIR spectroscopy of adsorbed pyridine on (×) ZβH, (+) ZβLi1, (■) Pt/ZβH and (♦) Pt/ZβLi2.

3.5. FTIR of adsorbed CO

FTIR of CO adsorbed on the solids showed the typical bands associated to CO linearly adsorbed on the metal (figure 3). The wave number of the CO vibration associated to CO adsorbed on Pt is shifted to lower wave numbers for the alkaline-exchanged supports. For Pt/ZβH the IR band appears at 2090 cm^{-1}, and for Pt/ZβCs this value was shifted to 2024 cm^{-1}. On the other hand, the catalyst Pt/ZβLi1 presented this band at 2063 cm^{-1}.

3.6. Catalytic activity

The activity and selectivity behavior of the catalyst Pt/ZβH as a function of temperature is shown in figure 4.

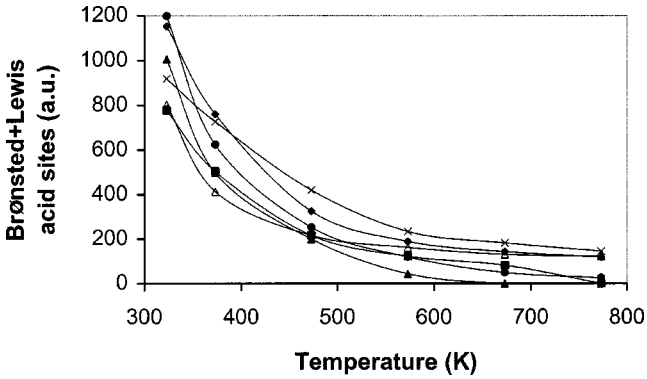

Figure 2. Brønsted + Lewis acid sites distribution determined by FTIR spectroscopy of adsorbed pyridine on (×) ZβH, (■) Pt/ZβH, (▲) Pt/ZβCs, (●) Pt/ZβLi1, (♦) Pt/ZβLi2 and (△) GAPt1.

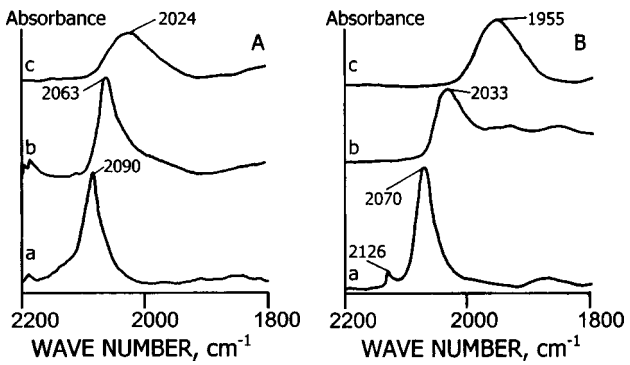

Figure 3. FTIR-CO spectra of platinum supported on (a) ZβH, (b) ZβCs and (c) ZβLi1 at (A) room temperature and (B) 473 K.

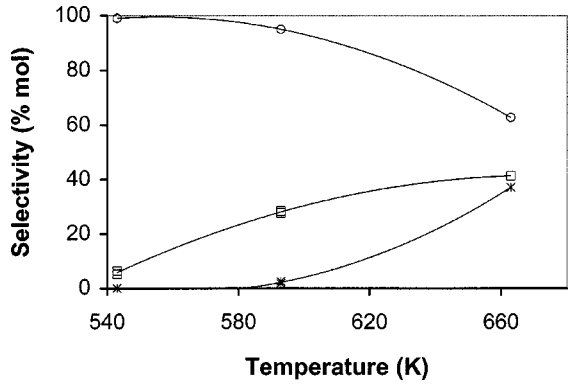

Figure 4. Catalytic selectivity of Pt/ZβH as a function of temperature: ($*$) aromatization, ($\circ$) isomerization and ($\square$) cracking.

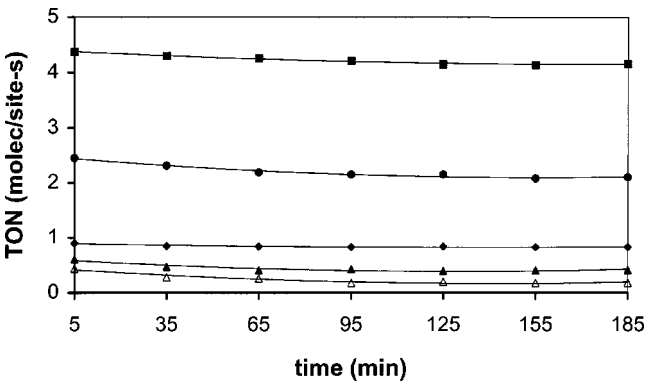

Figure 5. Catalysts activity vs. time calculated as turnover number (TON): (■) Pt/ZβH, (▲) Pt/ZβCs, (●) Pt/ZβLi1, (♦) Pt/ZβLi2 and (△) GAPt1.

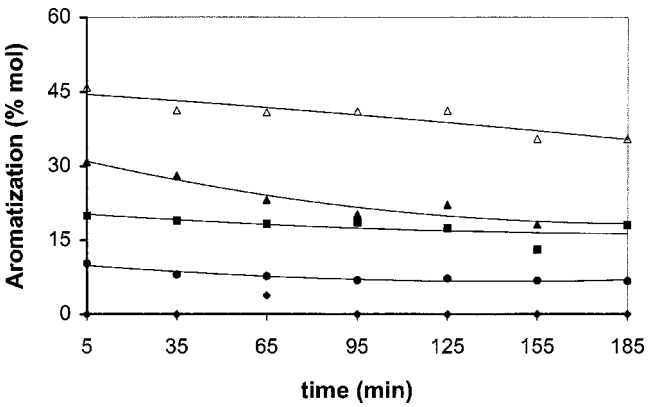

Figure 6. Catalysts selectivity (aromatization) vs. time: (■) Pt/ZβH, (▲) Pt/ZβCs, (●) Pt/ZβLi1, (♦) Pt/ZβLi2 and (△) GAPt1.

This behavior corresponds well with other reports [4–8], i.e., high isomerization levels at low temperatures and increased aromatization and cracking reactions as the temperature is increased.

The catalytic properties of the whole series of catalysts are summarized in figures 5–9; including the results of n-heptane conversion (turnover number, TON) and the data of selectivity versus time on stream. In table 2 a comparison is made for a time on stream of 95 min. From this comparison the following observations can be made.

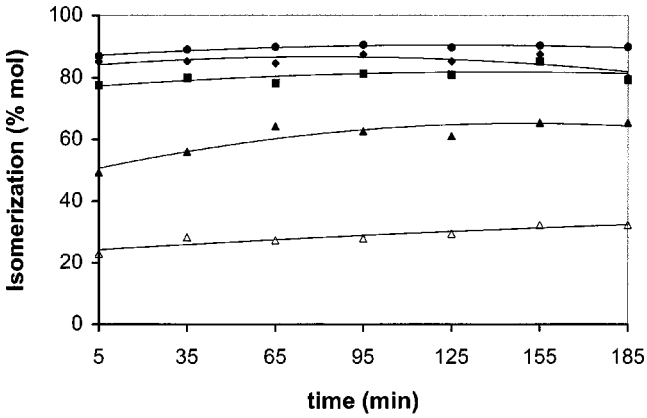

Figure 7. Catalysts selectivity (isomerization) vs. time: (■) Pt/ZβH, (▲) Pt/ZβCs, (●) Pt/ZβLi1, (♦) Pt/ZβLi2 and (△) GAPt1.

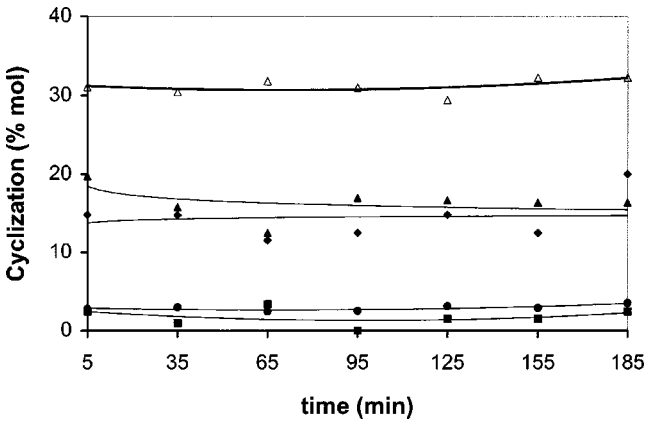

Figure 8. Catalysts selectivity (cyclization) vs. time: (■) Pt/ZβH, (▲) Pt/ZβCs, (●) Pt/ZβLi1, (♦) Pt/ZβLi2 and (△) GAPt1.

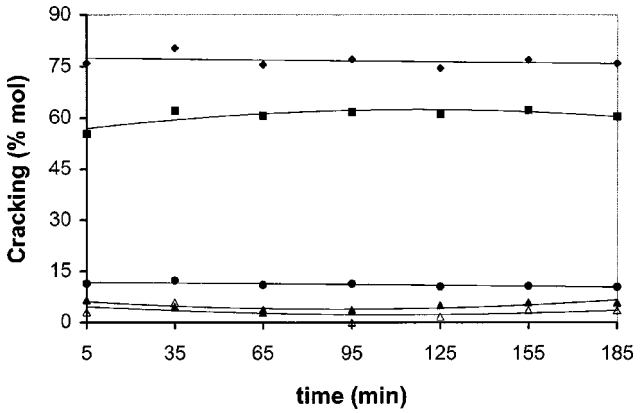

Figure 9. Catalysts selectivity (cracking) vs. time: (■) Pt/ZβH, (▲) Pt/ZβCs, (●) Pt/ZβLi1, (♦) Pt/ZβLi2 and (△) GAPt1.

The catalyst Pt/ZβH was the more active, the order of activity being as follows:

$$\text{Pt/Z}\beta\text{H} > \text{Pt/Z}\beta\text{Li1} > \text{Pt/Z}\beta\text{Li2} > \text{Pt/Z}\beta\text{Cs} > \text{GAPt1} > \text{CatCom.}$$

About 60% of the n-heptane converted on Pt/ZβH resulted in cracked products, due to its high number of acid sites

Table 2
Catalytic selectivity from n-C_7 conversion (mol%).[a]

Sample	TON (mol/site s)	Aromatization	Isomerization	Cyclization	Cracking	Acid/metal[b] ratio
Pt/Zβ H	4.21	18.7	81.3	0.0	61.8	30
Pt/Zβ Cs	0.43	20.3	62.7	17.0	3.7	7.8
Pt/Zβ Li1	2.15	6.9	90.5	2.6	11.4	24
Pt/Zβ Li2	0.83	0.0	87.5	12.5	77.1	45
GAPt1	0.18	41.1	27.9	31.0	0.0	24
CatCom	0.05	60.5	24.6	14.9	32.6	30

[a] Reaction conditions: 663 K, $P = 1$ atm, H_2/n-$C_7 = 50.5$ mol and 95 min on stream.
[b] Acid sites/Pt surface atoms.

Table 3
Product distribution from n-C_7 conversion (mol%).[a]

Sample	$C_3 + C_4$	C_6	$22dMC_5$	$23dMC_5$	$2MC_6$	$3MC_6$	$ECyC_5$	C_7	$MCyC_6$	Tol	Conversion
Pt/Zβ H	42.2	0.0	0.5	1.2	10.7	8.8	0.0	31.7	0.0	4.9	68.7
Pt/Zβ Cs	0.2	0.0	0.0	0.0	2.0	1.7	0.3	93.9	0.7	1.2	6.1
Pt/Zβ Li1	3.9	0.2	1.2	0.0	15.3	13.1	0.8	63.2	0.0	2.3	36.8
Pt/Zβ Li2	8.6	0.0	0.0	0.0	1.2	1.1	0.0	88.8	0.3	0.0	11.1
GAPt1	0.0	0.0	0.0	0.0	0.0	0.7	0.0	96.8	0.9	1.6	3.2
CatCom	0.4	0.4	0.0	0.0	0.3	0.1	0.3	97.5	0.0	1.0	2.4

[a] Reaction conditions: 663 K, $P = 1$ atm, H_2/n-$C_7 = 50.5$ mol and 95 min on stream.

(figure 9). The remaining 40% was comprised by isomerization followed by aromatization products. These results suggest that this catalyst is bifunctional having very active metallic and acid sites that promote the aromatization and isomerization reactions, as well as the reactions involving C–C bond rupture. The catalytic activity of Pt supported on zeolite was higher than the conventional reforming catalysts.

The comparison of selectivity for Pt supported on beta zeolite was as follows:

aromatization

$$\text{Pt/Z}\beta\text{Cs} \geqslant \text{Pt/Z}\beta\text{H} > \text{Pt/Z}\beta\text{Li1} > \text{Pt/Z}\beta\text{Li2};$$

isomerization

$$\text{Pt/Z}\beta\text{Li1} \approx \text{Pt/Z}\beta\text{Li2} > \text{Pt/Z}\beta\text{H} > \text{Pt /Z}\beta\text{Cs};$$

cracking

$$\text{Pt/Z}\beta\text{Li2} > \text{Pt/Z}\beta\text{H} \gg \text{Pt/Z}\beta\text{Li1} > \text{Pt/Z}\beta\text{Cs};$$

acid/metal ratio

$$\text{Pt/Z}\beta\text{Li2} > \text{Pt/Z}\beta\text{H} > \text{Pt/Z}\beta\text{Li1} > \text{Pt/Z}\beta\text{Cs}.$$

It is worth mentioning that the catalyst exchanged with cesium presented a marked selectivity towards aromatization and also the lowest yield of light alkanes.

The selectivity for these systems is displayed in table 3, where the following facts can be observed:

- The ratio 2-methylhexane/3-methylhexane was different from the typical ratio based on platinum sites.
- There is no formation of methane on any of the systems, i.e., the platinum was not able to promote hydrogenolysis reactions.

Table 4
Composition of the light products from n-C_7 conversion (mol%).[a]

Sample	C_2	C_3	i-C_4	n-C_4	i-$C_4 + n$-C_4	C_3/C_4
Pt/Zβ H[b]	0.2	23.9	28.6	9.1	37.7	0.63
Pt/Zβ H[c]	0.2	24.1	28.5	9.2	37.7	0.64
Pt/Zβ Li1[b]	0.0	4.0	5.1	2.0	7.1	0.56
Pt/Zβ Li1[c]	0.0	4.3	5.1	2.0	7.1	0.61

[a] Same experimental conditions as in tables 2 and 3.
[b] 95 min time on stream.
[c] 155 min time on stream.

- The only dibranched products were 2,2- and 2,3-dimethylpentane while the only aromatic product was toluene.
- The production of C_5 and C_6 alkanes was negligible.
- The light products were mainly propane, isobutane and n-butane.

The composition of the cracked products is presented in table 4. For Pt/Zβ H and Pt/Zβ Li1, the production of C_4 (i-$C_4 + n$-C_4) was higher than that of C_3, while the selectivity to i-C_4 was about three times higher than that to n-C_4 for Pt/Zβ H and two times higher for Pt/Zβ Li1. However, for both samples the C_3/C_4 ratio was very similar, i.e., $\sim$0.6.

The stability with time on stream was evaluated for Pt/Zβ H, and it is shown in figure 10, which shows that the loss of activity after 15 h of operation was less than 5%. In turn, the selectivity of the catalyst did not change along this interval, as shown in figure 11. Therefore, we are led to conclude that, under these experimental conditions there was no selective deactivation of the active sites of the catalysts.

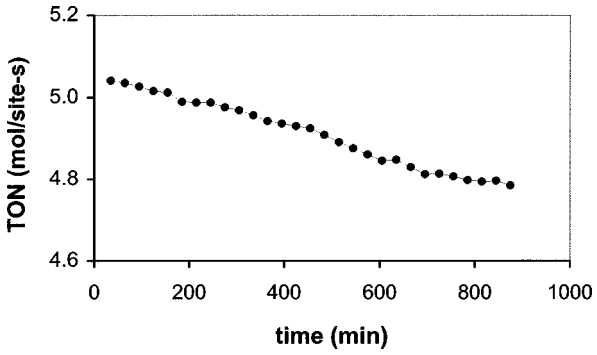

Figure 10. Catalytic stability of the Pt/ZβH catalyst: TON vs. time on stream.

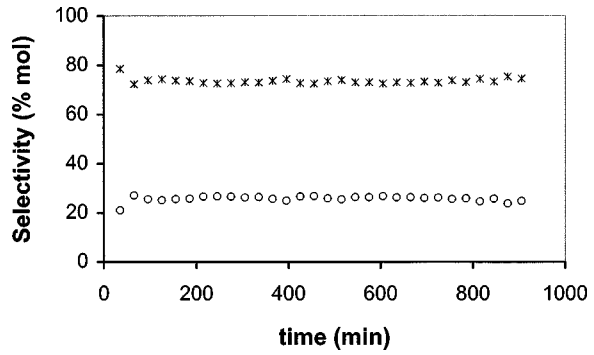

Figure 11. Catalytic selectivity of the Pt/ZβH catalyst vs. time on stream: (∗) aromatization and (○) isomerization.

4. Discussion

The $Pt(NH_3)_4(NO_3)_2$ ion-exchanged catalysts prepared in this work presented a high metal dispersion, i.e., Pt dispersion varied from 54% for Pt/ZβLi2 up to 81% for Pt/ZβLi1. The calcination step discards the possibility of auto-reduction of the platinum species. The high flow rate of the carrier gas (120 cm^3/min) used during this stage ensures the appropriate removal of water, allowing the displacement of the plane square complexes $[Pt(NH_3)_4]^{2+}$ to the interior of the channels network of the zeolite, as suggested by van der Broek et al. [17]. Although these authors based their studies on zeolite ZSM-5 that has a pore diameter of 5.4×5.6 Å, this phenomenon could be enhanced in beta zeolite due to its larger channel diameter, i.e., 6.8×7.3 Å.

The platinum dispersion data did not correlate directly with the content or type of cation (Cs or Li) exchanged in the beta zeolite, despite the fact that previous reports indicate a channel blockage effect on beta zeolite caused by the cesium cations [7,18]. It is important to mention that the X-ray diffraction patterns of the zeolites did not show a loss of crystallinity after the Cs and Li exchange [12].

All the Pt supported catalysts prepared on exchanged zeolites, i.e., Pt/ZβCs and Pt/ZβLi, showed an increase of their acid sites population (measured by NH_3-TPD) after the addition of platinum (table 1). In combination with the results from FTIR of adsorbed pyridine, we are led to conclude that this behavior is mainly caused by the presence of weak Lewis acid sites (figure 2).

Pt/ZβH did not present an important modification of its number of acid sites, as measured by NH_3-TPD and compared to ZβH, but it showed a decrease in its Brønsted acidity (figure 1). Therefore, $[Pt(NH_3)_4]^{2+}$ ions could be exchanged with protons on the zeolite.

Platinum supported on alumina (Pt/Al_2O_3) showed the presence of Lewis acid sites, which agrees with the intrinsic acidity of the alumina support.

In general, we can observe that the acid/metal ratio is of great importance to the behavior of these systems. For example, a small ratio results in high aromatization and isomerization but a low cracking of n-heptane, this being the case for Pt/ZβCs. Since the number of platinum active sites does not change substantially (i.e., fifth column of table 1), the acid/metal ratio depends mainly on the acid sites of the catalysts. As this ratio increases, the yield of light products also increases, due to the increase in the number of acid sites. Also, the catalysts having Brønsted acid sites produce more light products.

As observed, the activity of the cracking reaction followed the acid/metal ratio. The most active catalyst for isomerization was Pt/ZβLi, while Pt/ZβCs showed the highest selectivity for aromatization and cyclization and Pt/ZβLi2 was the most active catalyst for cracking.

Other authors [19] reported a higher cracking selectivity than the one reported here for Pt/ZβH under similar conditions. In this case, the main difference was the reaction temperature. While at 313 K they observed a selectivity for cracking around 86%, in this work, at 463 K, the selectivity was only 62%. Although in the present work the H_2/n-C_7 ratio was about seven times higher, this ratio must not be an important parameter at atmospheric pressure. Unfortunately in this paper [19] the Pt dispersion is not reported. These authors claim that under their reaction conditions a classical bifunctional mechanism takes place and reported a C_3/C_4 ratio close to 1, which validates their assumptions. In the present work this ratio was much lower, thus pointing out that the dimerization–cracking mechanism could be responsible for the excess of butane formed (table 4). Although we did not observe any products having five, six or a higher number of carbon atoms, the dimerization mechanism may be responsible for the distribution of the cracked products. Anyhow, the present distribution is a result of a complex mechanism for the hydrocracking of n-heptane which is explained in terms of the high level of conversion and temperature used in this work, [19,20]. The recombination of C_3 intermediates with n-C_7, and the further cracking of the resulting species, could explain the small C_3/C_4 ratio observed in this work.

Although the isomerization selectivity for Pt/ZβLi1 and Pt/ZβH catalysts varied only within 10%, their cracking selectivity varied up to 50%, which leads to considering that the isomers are formed and subsequently cracked. On the other hand, the Cs-exchanged catalysts presented the highest selectivity for aromatization, which might be related

to the basicity of the support and to the particular metal–support interaction.

An important result of the present work is the modification of selectivity upon cation exchange. The selectivity seemed to be sensitive to the electronic state of the metal, which is modified by the presence of the distinct alkaline cations that also provoke changes in the nature and amount of the acid sites. This interpretation is supported by the results of FTIR of adsorbed CO on the catalysts which may be explained in terms of an increased electronic density of Pt given by the interaction with the exchanged zeolite [21]. The frequency shift of the stretching vibration of CO is mainly due to the influence of the support on the force constant of the CO–Pt bond [22]. It was reported previously that the electronic density of platinum can be modified by the zeolite, causing a shift of the frequency of the stretching vibration of adsorbed CO [7,21,23]. In this sense, Cs- and Li-exchanged zeolites provoke important variations in the electronic state of platinum. Similar conclusions have been recently stated by Siffert et al. [23] using XPS of platinum supported on beta zeolite. They found that the platinum binding energy decreases when the basicity of the support increases, indicating an electron donation from the zeolite to the platinum. It has been reported that the close location of both the metal and the acid sites promotes the bifunctional mechanism [4] as well as the modification of the electronic density of the d orbitals of Pt [7,23]. However, the changes caused by the presence of alkaline cations on the metal properties seem significative, otherwise the results should be similar between Pt supported on the acidic zeolite and Pt supported on the exchanged zeolites.

Pt/ZβLi1 and GAPt1 catalysts presented very different catalytic properties (table 2), despite the facts that none of them had Brønsted acid sites, their Lewis and total acidity (figures 1 and 2) were very similar as well as their Pt contents and metal dispersion (table 2). This result supports the interpretation given by Smirniotis and Ruckenstein [4] about the closer contact between metal and acid sites in a zeolitic catalyst.

Therefore, the zeolitic support as well as the nature of the exchanged cations produce changes in the selectivity of supported Pt catalysts for n-C_7 reforming type reactions. The modification of the electronic density of Pt induced by the presence of alkaline cations in the support may lead to metal–support interactions, resulting in the variation of the catalytic properties of Pt/ZβM with respect to conventional Pt/γ-alumina and Pt/ZβH catalysts.

5. Conclusions

In this study several catalysts of platinum supported on beta zeolite (acid and exchanged with Cs and Li) were prepared and presented different catalytic properties according to the type and concentration of the exchanged cations. The characterization of the metallic phase and the support led to the conclusion that there is an interaction between them. Catalysts with high metal dispersion and different number of acid sites were obtained. A close relation was found between the cracking selectivity and the acid/metal ratio. The IR study showed a displacement of the CO frequency (ν_{CO}) in the Pt supported on the exchanged solids, i.e., Pt/ZβM with respect to Pt/ZβH. These frequency shifts were interpreted in terms of the strong interaction that takes place between the alkaline metals in the support and the metallic phase (Pt), which provokes the shift of the IR bands due to the electron donation from the support to the metal particle. This, in turn, influences the catalytic properties of the active phase, showing that Pt/ZβCs promotes aromatization rather than the isomerization reactions.

Acknowledgement

SR highly appreciates the economical support from the Instituto Mexicano del Petróleo for his graduate studies.

References

[1] J.R. Bernard, in: *Proc. 9th Int. Zeol. Conf.*, Naples, ed. L.V.C. Rees (Heyden, London, 1980) p. 686.
[2] N.Y. Chen and T.F. Degnan, Chem. Eng. Prog. 88 (1988) 32.
[3] I.E. Maxwell, Catal. Today 1 (1987) 385.
[4] P.G. Smirniotis and E. Ruckenstein, J. Catal. 140 (1993) 526.
[5] H. Yue Chu, M.P. Rosynek and J.H. Lunsford, J. Catal. 178 (1998) 352.
[6] J. Zheng, J.L. Dong, Q.H. Xu, Y. Liu and A.Z. Yan, Appl. Catal. A 126 (1995) 141.
[7] T. Bécue, F.J. Maldonado-Hódar, A.P. Antunez, J.M. Silva, M.F. Ribeiro, P. Massiani and M. Kermarec, J. Catal. 181 (1999) 244.
[8] T. Fukunaga and V. Ponec, Appl. Catal. A 154 (1997) 207.
[9] J.A. Martens and P.A. Jacobs, Stud. Surf. Sci. Catal. 58 (1991) 445.
[10] E. Blomsma, J.A. Martens and P.A. Jacobs, J. Catal. 165 (1997) 241.
[11] N.Y. Chen, W.E. Garwood and F.G. Dwyer, *Shape Selective Catalysis in Industrial Applications* (Dekker, New York, 1989) p. 157.
[12] S. Ramírez, J.M. Domínguez, M. Viniegra and L.Ch. de Ménorval (1999), submitted.
[13] C.A. Emeis, J. Catal. 141 (1993) 347.
[14] W.A. Dietz, J. Gas Chromatogr. 71 (1967) 68.
[15] J.C. Rasser, *Platinum–Iridium Reforming Catalysts* (Delft University Press, Delft, 1977).
[16] S. Siffert, D.Y. Murzin and F. Garin, Appl. Catal. A 178 (1999) 85.
[17] A.C.M. van den Broek, J. van Grondelle and R.A. Santen, J. Catal. 167 (1997) 417.
[18] F.J. Maldonado-Hódar, M.F. Ribeiro, J.M. Silva, A.P. Antunez and F.P. Ribeiro, J. Catal. 178 (1998) 1.
[19] Z.B. Wang, A. Kamo, T. Yoneda, T. Komatsu and T. Yashima, Appl. Catal. A 159 (1997) 119.
[20] A. Lugstein, A. Jentys and H. Vinek, Appl. Catal. A 166 (1998) 29.
[21] A. Besoukhanova, J. Guidot, D. Barthomeuf, M. Breysse and J.R. Bernard, J. Chem. Soc. Faraday Trans. 77 (1981) 1595.
[22] M. Primet, J.M. Basset, M.V. Mathieu and M. Prettre, J. Catal. 29 (1973) 213.
[23] S. Siffert, J.L. Schmitt, J. Sommer and F. Garin, J. Catal. 184 (1999) 19.